International Core Journal of Engineering Volume 5 Issue 10, 2019
ISSN: 2414-1895 DOI: 10.6919/ICJE.201909_5(10).0032

DC Bus Voltage Adaptive Control for DC Microgrid with Wind Power Generator Systems

Linjin He

School of Logistics Engineering, Shanghai Maritime University, Shanghai 201306, China;

helinjin0120@hotmail.com

Abstract

This paper studies the DC microgrid in island mode established by permanent magnet direct-drive wind power generation. When the load is abrupt, the output power rate of the wind turbine is controlled to match the load power variation, and the DC bus voltage drop is reduced. Based on the analysis of the relationship between wind turbine output power, DC bus capacitor energy storage and load power energy, a hybrid adaptive control algorithm is proposed to achieve the maximum wind turbine power change rate by searching for the optimal generator acceleration. Therefore, the load power variation is matched, and the difference between the load power and the generator output power is reduced, thereby reducing the DC bus voltage drop and maintaining the bus voltage stability. A 1.5MW wind power simulation system was established to verify the effectiveness of the control algorithm.

Keywords

Wind power generation; permanent magnet synchronous generator; DC microgrid; adaptive control.

1. Introduction

Today, in wind power DC grid-connected research, permanent magnet synchronous generators (PMSG) are increasingly incorporated into DC-microgrids via PWM converters because of their high power density and simple control. The DC bus voltage of an electric DC microgrid is usually controlled by a grid-side converter, and the wind turbine side converter obtains maximum power tracking (MPPT) by adjusting the speed of the generator[1, 2, 3].

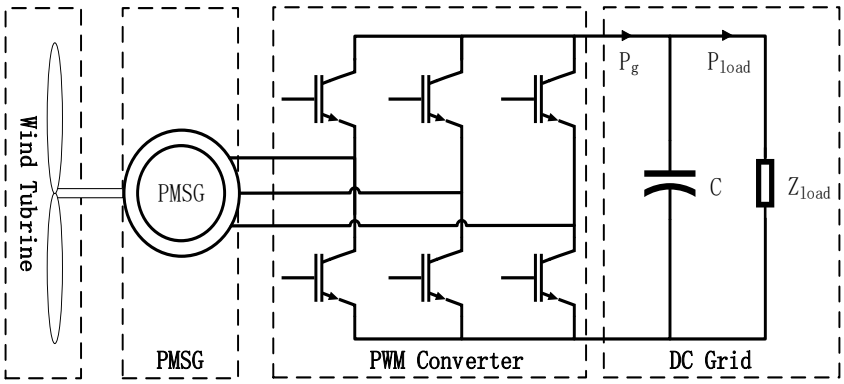

Fig. 1 Direct drive wind power DC microgrid structure

ISSN: 2414-1895 DOI: 10.6919/ICJE.201909_5(10).0032

When the wind power DC microgrid system is in the grid weak connection mode or island mode, and the wind power generation is its main energy source or a single energy source(The overall structure of the direct drive wind power DC microgrid system is shown in Fig 1.), the machine side converter assumes the function of maintaining the DC bus voltage and active balance. The basic principle of the machine-side converter for DC bus voltage control is to balance the load power by adjusting the generator output power to maintain the DC bus voltage balance [4,5]. The speed-power nonlinearity of the wind turbine makes the control of the DC bus voltage very challenging. In a low-power wind power generation system, during the load change process, the excess active power can be consumed by the chopper circuit in parallel with the resistor, and the DC bus voltage is kept constant, while in high-power wind power systems, there is no practical application due to excessive energy loss.

To this end, this paper focuses on the wind power DC micro-grid in the island mode [6, 7], DC load voltage control through the PWM converter when the load is widely fluctuated. The control unit side converter changes the generator speed, changes the wind turbine output power to match the load power change and maintains the DC bus voltage constant. The energy relationship between the wind turbine, the permanent magnet synchronous generator, the DC link capacitor and the load is established. The analysis found that the inherent half-plane zero of the system, the nonlinear characteristics of the wind turbine, the mechanical inertia of the system and the energy storage of the DC link limit the DC bus voltage constant during load fluctuations. A hybrid adaptive PI is proposed. The control algorithm obtains the maximum rate of change of the generator output power by searching for the acceleration of the optimal PMSG, thereby quickly balancing the fluctuation of the DC bus voltage due to load changes.

2. Proposed Control Method

2.1 Basic Control Principle and Requirements

Wind Turbine and PMSG

Betz's law shows that the mechanical power of the wind turbine shaft output is [8,9]. In this paper, the pitch angle(β) is first assumed to be fixed at 0◦ for the simplicity of analysis.

$$P_w = \frac{1}{2}\rho A C_p(\omega,\beta)\upsilon^3 . \tag{1}$$

where ρ is the air density, A is the wind turbine swept area($A=\pi*R^2_w$), υ is the wind speed, and C_p is the power coefficient of the wind turbine and a function of the turbine (or generator) speed ω.

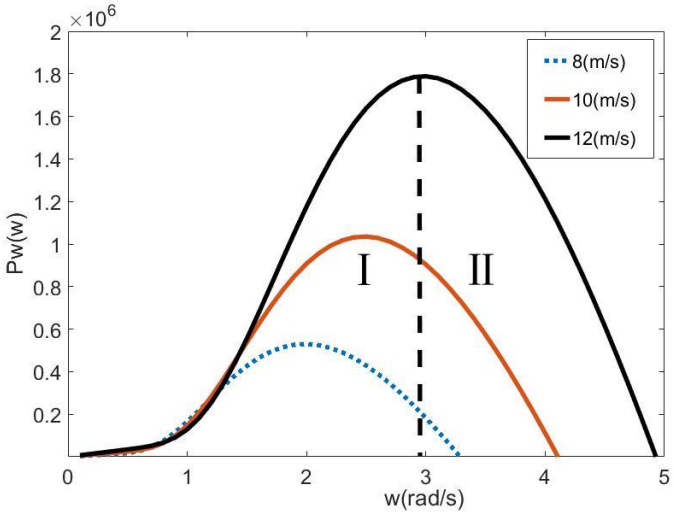

Fig. 2 Wind power–speed characteristics for a 1.5-MW system

ISSN: 2414-1895 DOI: 10.6919/ICJE.201909_5(10).0032

Under the determination of the wind speed υ, the relationship between the output mechanical power P_w and the wind turbine angular velocity ω on the wind turbine shaft is as shown in Fig. 2 [10], The curves are divided into two regions with a positive slope (I) and a negative slope (II).

The mathematical model of the permanent magnet synchronous generator (PMSG) in the rotating coordinate system [11] can be expressed as

$$\begin{aligned} v_d &= -Ri_d - L_d \frac{di_d}{dt} + L_q \omega_e i_q \\ v_q &= -Ri_q - L_q \frac{di_q}{dt} - L_d \omega_e i_d + \omega_e \psi \end{aligned} \tag{2}$$

Where v_q, v_q, i_d, i_q is the PMSG stator voltage and current in the rotating coordinates, L_d, L_q is the stator direct axis and the cross-axis inductance, R is the generator stator armature resistance, ω_e is the electrical angular velocity, and ψ is the permanent magnet flux linkage.PMSG power generation electromagnetic torque is

$$T_e = \frac{3}{2} n_p [\psi i_q + (L_d - L_q) i_d i_q] \tag{3}$$

In the case of PMSG ($L_d = L_q$) with a surface-mounted structure, the electromagnetic torque equation can be simplified to

$$T_e = \frac{3}{2} n_p \psi i_q \tag{4}$$

Where: n_p is the motor pole logarithm.

Basic Control Principle

The basic control principle is illustrated in Fig. 3. As can be seen in Fig. 3, in order to maintain the DC bus voltage, the generator output power P_g should track the load power demand P_{load}, which can be achieved through controlling the generator speed based on the power–speed characteristics of the wind turbine.

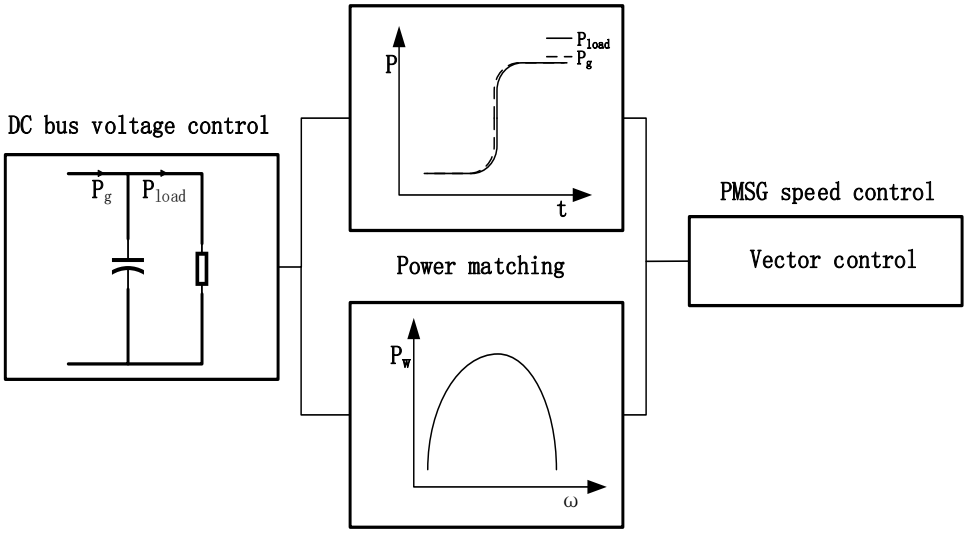

Fig. 3 DC bus voltage control schematic

Neglecting the power converter losses, the dynamic equation of the DC bus voltage can be written as in (2), where V_{dc} and i_{dc} are the voltage and current of the dc-link capacitor, respectively

ISSN: 2414-1895 DOI: 10.6919/ICJE.201909_5(10).0032

$$P_{\mathrm{g}} - P_{\mathrm{load}} = V_{\mathrm{dc}} i_{dc} = V_{\mathrm{dc}} C \frac{dV_{dc}}{dt} . \tag{5}$$

Practically, P_g is equal to P_w at steady state without considering losses. During PMSG speed change, P_g differs with P_w by the required mechanical power for acceleration or deceleration, as shown in (6), where J is the system inertia and generator losses (electrical and mechanical) are neglected

$$P_w - P_{\mathrm{g}} = J\omega \frac{d\omega}{dt} \tag{6}$$

From (5) and (6), it is clear that one option to control the DC bus voltage is to change the generator output power P_g by controlling the generator speed. In order to obtain the relationship between the DC bus voltage V_{dc} and the generator speed ω, (1) ,(5),(6) can be combined to yield the following equation:

$$\frac{1}{2}\rho A C_p(\omega)\upsilon^3 - V_{\mathrm{dc}} C \frac{dV_{dc}}{dt} - P_{\mathrm{load}} = J\omega \frac{d\omega}{dt} \tag{7}$$

Considering P_{load} as the disturbance,(7) can be linearized at a given operating point (e.g., DC bus voltage V_{dc0}, PMG speed ω_0, and wind speed υ_0). The transfer function of the DC bus voltage $V_{dc}(s)$ and generator speed $\omega(s)$ is then described by the frequency-domain model in (8), where k is the slope of the curve in Fig. 2 corresponding to the operating point:

$$\frac{V_{dc}(s)}{\omega(s)} = \frac{k - J\omega_0 s}{V_{dc0} C s} = \frac{J\omega_0}{V_{dc0} C} \frac{J\omega_0(-s + (k / J\omega_0))}{s} \tag{8}$$

As can be seen in Fig. 3, if the generator is operating in sector I, then k > 0 and the system will have an right-half-plane zero(RHZ). This RHZ will add control complexity and limit the system performance.On the other hand, in sector II, k < 0 and the transfer function will have a left-half-plane zero (LHZ), which tends to be easier to deal with in control design. For a given power level, the PMSG can operate at two speed points in sector I or II, as seen in Fig. 2. While it may be preferable to operate the turbine/generator in a particular sector for a particular application requirement (e.g., sector I for lower speed—thus lower mechanical loss and stress; sector II for higher stored kinetic energy capability), the control design ought to consider both sectors as the operating point can jump from one sector to the other during a fast wind speed or load change. Given the presence of the RHZ and other complexities associated with sector I, this paper will mainly focus on controller design for sector I. The design for sector II can follow the same procedure.

Based on the aforementioned analysis, the DC bus voltage control during the island mode can be realized through the basic controller structure in Fig. 4. A DC bus voltage control loop can be used to generate the required PMSG speed reference .

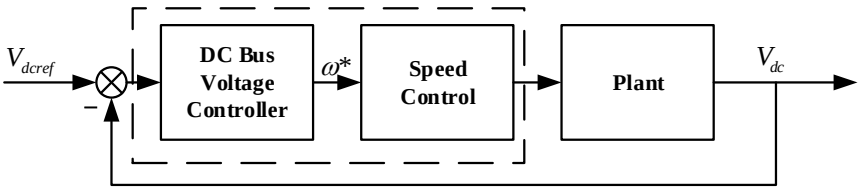

Fig.4 DC bus voltage control structure diagram

The speed control can be implemented similarly as PMSG control in the normal strong grid connected.By changing the generator speed , the wind power will change according to Fig. 2 , and

ISSN: 2414-1895 DOI: 10.6919/ICJE.201909_5(10).0032

will change with via (6) to compensate for the load power change, thus keeping DC bus voltage regulated(Generally, the DC bus voltage deviation is allowed to be ±10% of the rated DC bus voltage).

Control Performance Analysis

A simple proportional–integral (PI) regulator can be used for implementing the dc-link voltage controller in Fig. 4.

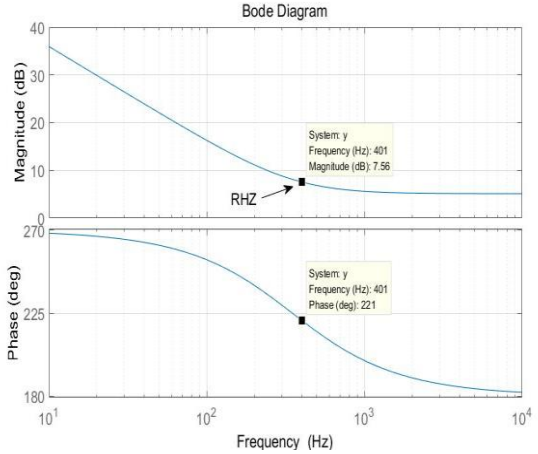

Fig.5 Openloop frequency response without compensator

We use the same 1.5MW system as depicted in Fig. 2, which operates in sector I, ($C = 200mF, V_{dc0} = 700V, J = 100kg/m^2, \upsilon_0 = 12m/s, \omega_0 = 2.55rad/s, k = 5.6\times10^5 N.m$),The corres--ponding RHZ is at 401 Hz.Fig.5 shows the open-loop frequency response curve when the system is uncompensated. Since the crossing frequency can only be selected before the corresponding frequency of the right half-plane zero to ensure system stability, the control performance of a simple PI controller based on one operating point is limited.

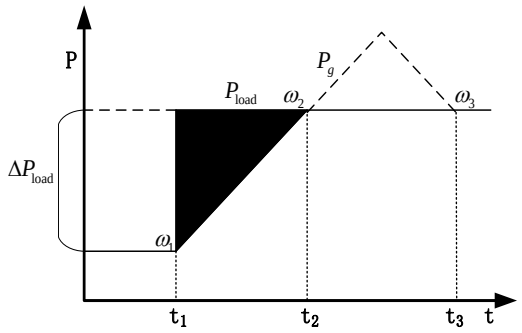

Fig.6 System power relationship analysis diagram

The DC bus voltage change is the result of sudden load change. Assume that at $t = t_1$, the wind speed remains the same and the load power is increased by ΔP_{load} from P_{load}. As shown in Fig.6, it can be seen from Fig.2 that the Turbine/PMSG speed ω is rising, increasing the wind turbine output power P_w to meet the load power requirement. During this acceleration, part of the power is converted into the mechanical energy related to the system energy storage P_{mec} ($P_{mec} = J\omega d\omega/dt$) due to the inertia of the system, and the remaining part is converted into the power of the PMSG output P_g (Feed by the PWM converter to the DC bus). It can be seen from Fig.1that even if the rise in the section I causes the P_w to increase, the PMSG cannot accelerate too fast, otherwise the majority of P_w will be converted to P_{mec} due to the excessive $d\omega/dt$, thereby making the P_g smaller.

ISSN: 2414-1895 DOI: 10.6919/ICJE.201909_5(10).0032

Therefore, when the Wind Tubrine is operating in the section I, the angular velocity is changed to cause an increase in P_w and an increase in P_{mec}. There is an optimum acceleration $d\omega/dt$, so that P_g can be kept maximum when the load power is increased. The shaded energy shown in Figure 6 is the difference between P_w and P_g that the DC bus storage capacitor needs to compensate, which is also the cause of the bus voltage drop.

Table 1 Direct Drive Wind Power DC Microgrid System Parameter

Tubrine	Parameter	PMSG	Parameter
R_w(m)	31.9	R_s(mΩ)	60
ρ(kg/m^3)	1.29	L_d、L_q(mH)	0.2
C(mF) V_{dc}(V)	200 700	ψ n_p J (kg/m2)	1.029 98 100

To simplify the analysis, (assuming dP_w/dt and acceleration $d\omega/dt$ are set to constant, $dP_w/dt = k$, $d\omega/dt = k_1$). The rates of change of P_w and P_{mec} are as shown in equations (9a) and (9b), respectively. The difference between them is the rate of change P_g (10)

$$\frac{dP_w}{dt} = \frac{dP_w}{d\omega}\frac{d\omega}{dt} = kk_1 \tag{9a}$$

$$\frac{dP_{mec}}{dt} = \frac{d(\omega J\, d\omega/dt)}{dt} = k_1^2 J \tag{9b}$$

$$\frac{dP_g}{dt} = \frac{d(P_w - P_{mec})}{dt} = kk_1 - k_1^2 J \tag{10}$$

It can be seen from equation (10) that the maximum power change rate is mainly determined by the Wind Tubrine speed-power curve slope k and the system inertia J. When the load power increases, the larger k corresponds to a larger power change rate.

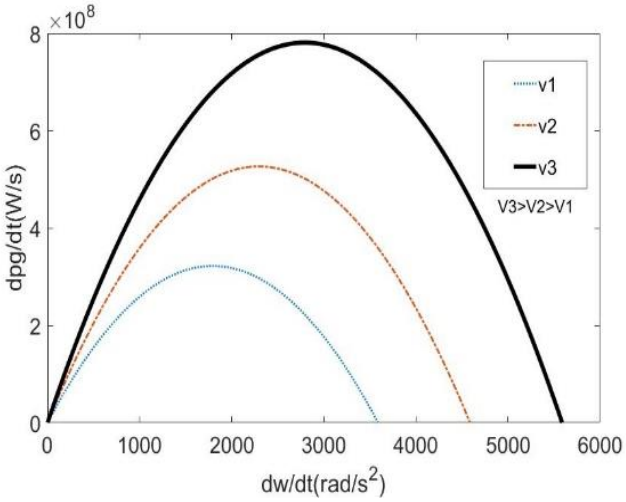

Fig.7 output power change rate and angular velocity change rate

ISSN: 2414-1895 DOI: 10.6919/ICJE.201909_5(10).0032

At this time, the DC bus voltage drop recovery time is shorter, while the larger J corresponds to more system energy storage and less PMSG output power. Feedback to the DC bus. Equation (10) shows that after the system parameters are determined (k， J determined), k_1 can be controlled to obtain the maximum dP_g/dt. It can be seen from Fig. 7 that there is always an optimal $d\omega_{optimal}/dt$ such that $dP_{g(\max)}/dt$, the maximum dP_g/dt corresponds to the minimum DC bus voltage drop when the wind speed ($V_3>V_2>V_1$) is different, so the controller is designed to search for the optimal $d\omega/dt$, thereby reducing the voltage drop.

Using the same assumptions as shown in Figure 6, when the load power is increased ΔP_{load} at $t = t_1$, the generator output power P_g will rise at the $k_2 = dP_g/dt$ as shown in equation (10), and the output power will reach the load power at time $T=(t_2-t_1)=\Delta P_{\text{load}}/k_2$, the DC bus voltage drop is caused by the energy difference between the generator output power and the load power. The energy E_c expression is shown in (11), and the simultaneous (11) and capacitive charge relationship is available (12).

$$E_c=\frac{1}{2}\Delta P_{\text{load}}T=\frac{1}{2}\frac{\Delta P_{\text{load}}{}^2}{k_2} \tag{11}$$

$$\frac{1}{2}CV_{dc}{}^2(t_1)-\frac{1}{2}CV_{dc}{}^2(t_2)=\frac{1}{2}\frac{\Delta P_{\text{load}}{}^2}{k_2} \tag{12}$$

The required capacitance value is obtained in consideration of the DC bus voltages $V_{dc}(t_1)-V_{dc}(t_2)$ and ΔP_{load}.

$$C=\frac{\Delta P_{\text{load}}{}^2}{k_2(V_{dc}{}^2(t_1)-V_{dc}{}^2(t_2))} \tag{13}$$

Under the condition of $\Delta P_{\text{load}}=300\text{kW}$ and initial voltage $V_{dc}(t_1)=700\text{V}$, use the system parameters of Table 1 and select capacitor $C=200mF$ to handle transient load changes. This conclusion applies to the case of load power drop and voltage rise.

Note that the dc-link capacitance values on the order of hundreds of millifarads, required for energy storage, seem to be excessive compared with the values used in other converter applications, for the same power rating.but based on the size of commercial electrolytic capacitor capacitor banks, this is approximately It is not unreasonable for 1.5MW wind power generation.

2.2 Hybrid Adaptive PI Control.

The control structure of the DC bus voltage controller is shown in Figure 4. The controller is designed to obtain the maximum dP_g/dt.The controller is designed to obtain the maximum dP_g/dt. For the small-signal model of a given operating point, the established PI (PI parameter is constant) controller can only obtain the corresponding control performance near this point. When the load fluctuates widely, the control performance decreases, resulting in a large range of DC bus voltage. Deviate and recover longer. In order to optimize system performance during large-scale load fluctuations, a hybrid adaptive PI control algorithm based on energy and power relationship is proposed.

The purpose of the hybrid adaptive PI control algorithm is to find the optimal $d\omega/dt$, obtain the maximum dP_g/dt, and reduce the bus voltage drop. The basic working principle of the controller is as follows:

ISSN: 2414-1895 DOI: 10.6919/ICJE.201909_5(10).0032

1. Controller input ΔP_w, $\Delta\omega$, determine the system working area by formulas (14), (15), (16). When the system runs in area II, maintain the DC bus voltage stability through a simple PI controller; the system runs in area I. The DC bus voltage is stabilized by the adaptive PI controller.

$$\begin{aligned}\Delta P_w &= P_{w(k)} - P_{w(k-1)} \\ \Delta\omega &= \omega_{(k)} - \omega_{(k-1)}\end{aligned} \tag{14}$$

$$\begin{aligned} signP &= \begin{cases} 1 & \Delta P_w > 0 \\ -1 & \Delta P_w < 0 \end{cases} \\ sign\omega &= \begin{cases} 1 & \Delta\omega > 0 \\ -1 & \Delta\omega < 0 \end{cases}\end{aligned} \tag{15}$$

$$\begin{aligned} signP*sign\omega > 0 \quad & \text{section I} \\ signP*sign\omega < 0 \quad & \text{section II}\end{aligned} \tag{16}$$

2. When the system is running in area I, the controller inputs ΔV_{dc}, ΔP_g, V_{dcn} (rated voltage of DC bus), determines the operating point of system angular velocity change rate by formulas (17), (18), (19), and changes PI according to working point. The part of controller K_p that changes $d\omega/dt$ and looks for the largest dP_g/dt.

$$\begin{aligned}\Delta V_{dc(k)} &= \left|V_{dc(k)} - V_{dcn}\right| \\ \Delta P_{g(k)} &= P_{g(k)} - P_{g(k-1)} \\ \Delta P_{g(k-1)} &= P_{g(k-1)} - P_{g(k-2)}\end{aligned} \tag{17}$$

$$\Delta K_p = \begin{cases} 0 & \Delta V_{dc} < \Delta \\ K_p & \Delta V_{dc} > \Delta \end{cases} \tag{18}$$

$$\begin{cases} \left|\Delta P_{g(k)} - \Delta P_{g(k-1)}\right| > 0 & K_{p(k+1)} = K_{p(k)} + \Delta K_p \\ \left|\Delta P_{g(k)} - \Delta P_{g(k-1)}\right| < 0 & K_{p(k+1)} = K_{p(k)} - \Delta K_p \end{cases} \tag{19}$$

The control algorithm needs to make the DC bus voltage deviate within $\pm 10\% V_{dcn}$. When the error $\left|\Delta V_{dc}\right| < \Delta$, the PI controller remains constant (constant). The proposed DC bus voltage hybrid adaptive PI controller flow chart is shown in Fig.8, where $\Delta = 5\% V_{dcn}$, K_p = 0.01. Through the small-signal model analysis, as shown in the system response curve shown in Fig.5, the PI controller is set to $K_p = 1, K_i = 5$ near the operating point so that its crossing frequency is 0.99 Hz and the phase margin is 45^o.

When the DC bus deviation $\left|\Delta V_{dc}\right| > 2.5\% V_{dcn}$, the PI controller parameters are adaptively changed to improve the dynamic performance of the system, each control cycle is incremented or decreased by 0.01 in steps to change the PMSG acceleration rate, The DC bus voltage variation is reduced, wherein the DC bus voltage control period is much larger than the speed/torque inner loop.

As K_p gradually increases, the proportion of the DC bus voltage PI control will increase accordingly. Depending on the polarity of the voltage deviation, a larger or smaller speed reference ω^* will be produced. For positive polarity error (voltage dip), a larger ω^* pass speed/torque control will cause the PMSG speed to increase faster, ie $d\omega/dt$ larger; For negative polarity error (voltage rise), a smaller ω^* speed/torque control will cause the PMSG speed to decrease faster, ie, the negative

ISSN: 2414-1895 DOI: 10.6919/ICJE.201909_5(10).0032

$d\omega/dt$ is larger, both cases make $\left|dP_g/dt\right|$ larger and increase until $\left|dP_g/dt\right|$ It is the maximum value, which corresponds to the maximum power change rate and the optimal speed change rate.

For DC bus voltage regulation, the external loop voltage controller needs to be used with the internal speed controller, as shown in Figure 4.

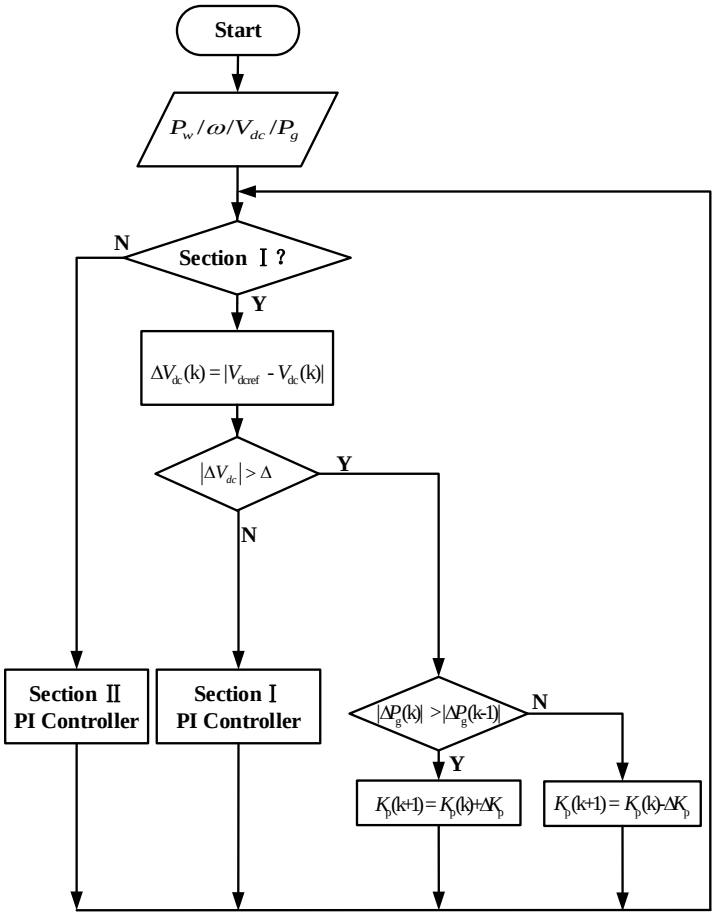

Fig.8 Hybrid Adaptive PI Control Flowchart

The speed/torque control using vector control in this paper is shown in [12]. It can be seen from [12] that the torque of the PMSM is controlled by the q-axis current, and the d-axis current component is mainly used to obtain a unit power factor, thereby obtaining the minimum power loss and the maximum available torque. Ignoring converter losses, the generator and converter output power can be expressed as

$$P_g = \frac{3}{2}(v_d i_d + v_q i_q) \tag{20}$$

3. Simulation

In order to verify the effectiveness of the control method proposed in this paper, hybrid adaptive PI control and PI control method are adopted on Matlab/Simulink respectively, and the DC bus voltage of wind power DC microgrid is changed for different wind speeds and different working areas. The control structure of the established 1.5MW wind DC microgrid system (parameters shown in Table 1) is shown in Figure 4.

The simulated wind speed-power-speed curve is shown in Figure 3. The constant power load is assumed to range from 0 to 1.5 MW on the DC bus. The steady state conditions are the same as in Table 1($C = 200mF, V_{dc0} = 700V, P_{load} = 1400kW, \upsilon_0 = 12m/s$， ω_0=2.55rad/s， $k = 5.6\times10^5 N.m$).

ISSN: 2414-1895 DOI: 10.6919/ICJE.201909_5(10).0032

The compensation system crossover frequency is chosen to be $f_0 = 0.99Hz$ to have a 45^o phase margin. The corresponding proportional and integral gains of the PI controller are $K_p = 1, K_i = 5$.

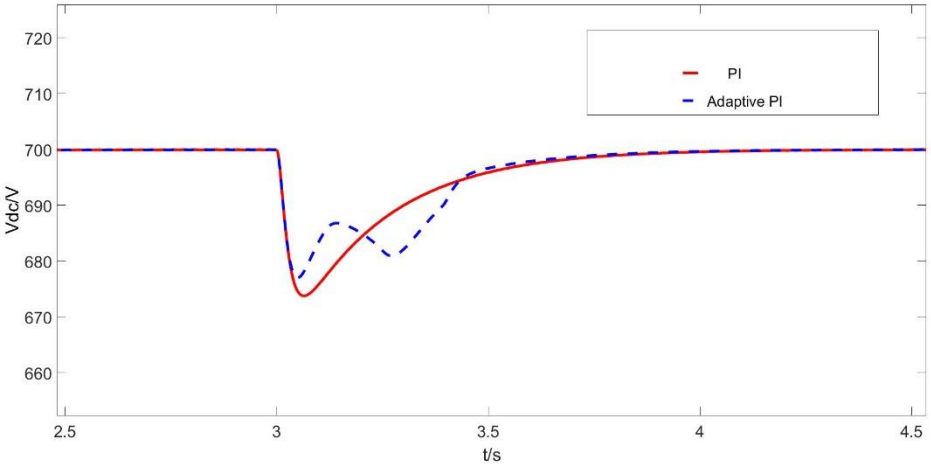

Fig.10 (a) DC bus voltage change

The PI parameter selection has a certain margin to adapt to other conditions (wind speed, PMSG speed, load, etc.). The speed and torque/current controller controller bandwidth is wider than the DC bus voltage controller bandwidth, and the adaptive controller has little practical impact on system dynamics due to large load changes.

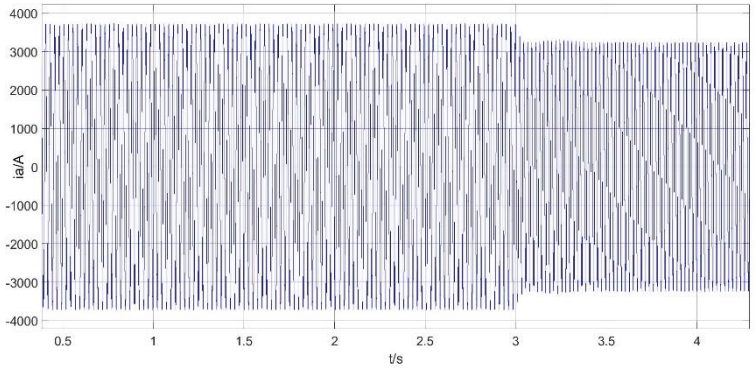

Fig.10(b) PMSG stator current

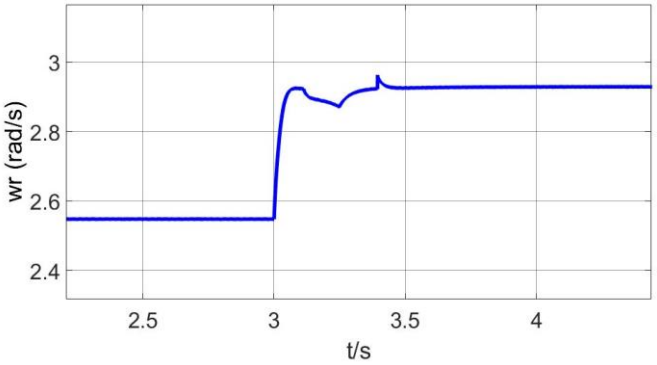

Fig.10(c) PMSG angular velocity

For a constant wind speed of 12 m / s, some simulation results obtained are shown in Fig.10: (a) DC bus voltage change observed after applying a load step of 200 kW to 500 kW at time t = 3 s, DC bus voltage The rated value is 700 V; (b) i_a the phase current of the generator during this dynamic change; (c) w_r the angular velocity of the wind turbine when the load power increases; the PMSG reference speed and the actual speed increase during the dynamic change of the section I, and the

ISSN: 2414-1895 DOI: 10.6919/ICJE.201909_5(10).0032

angular velocity is adjusted by the PMSG To compensate for load power variations, the DC bus voltage is well regulated within acceptable voltage drop limits.

The load mutation simulation results show that compared with the traditional PI control method, the adaptive PI control can significantly reduce the bus voltage drop and the bus voltage recovery time is shorter.

4. Conclusion

This paper studies the DC bus voltage control strategy of direct-drive wind power DC microgrid, analyzes the power and energy relationship of wind power DC micro-grid composed of wind turbine, permanent magnet synchronous generator and PWM converter, and establishes the PMSG speed and The relationship between the DC bus voltages. When the load in the microgrid system is abrupt, the hybrid adaptive PI control strategy proposed in this paper can maintain the stability of the DC bus voltage by controlling the PMSG speed. The simulation results also show that the proposed control strategy can achieve DC bus stability, which provides a theoretical value for the future research of direct-drive wind power into DC Microgrid.

References

[1] Hui Jing, Fang Guanghui: New Energy Conversion and Control Technology (Mechanical Industry Press, China 2008). (In Chinese)

[2] Lin Weiwei, Wen Buzhen. Review of the impact of large-scale wind power access on power system transient stability. Electric Technology, 2017(04): 1-8+38. (In Chinese)

[3] Y. Zhang, X. Han, B. Xu, M. Wang, P. Ye, and Y. Pei, Risk-based admissibility analysis of wind power integration into power system with energy storage system ,IEEE Access, vol. 6, pp. 57400–57413, 2018.

[4] Xibo Yuan,Yongdong Li,Control of variable pitch and variable speed direct-drive wind turbines in weak grid systems with active power balance,Renewable Power Generation IET,vol. 8,no.2,pp.119-131,2014.

[5] Yuan,X.,Wang,F.,Borojevich,D.“DC-link voltage control of full power converter for wind generator operating in weak grid systems”, IEEE Trans. Power Electron. 2009, 24, (9), pp.2178–2192

[6] ZHAO Yong,ZHANG Defu.Inverter Grid-connected and island mode seamless switching model predictive control.Power Electronics Technology,2019,53(03):42-46.(In Chinese)

[7] Sun Ao. Research on smooth switching control strategy of microgrid. Xinjiang University, 2017. (In Chinese)

[8] Wu Aihua,Zhao Bianbo,Mao Jingfeng.Power Sliding Mode Control of Permanent Wind Direct Drive Wind Power Generation System in Full Wind Condition.Journal of System Simulation,2016,28(01):99-105. (In Chinese)

[9] Chen Jie, Gong Chunying,Full Range Power Control Strategies for Variable-speed Fixed-pitch Wind Turbine,Proceedings of the CSEE, vol. 32, no. 30, pp. 98-104, 2012.

[10] Geng Chenjing,Zhang Huijuan.Simulation Research on Maximum Power Point Tracking Control Optimization in Permanent Magnet Direct Drive Wind Power System.Motor and Control Applications,2017,44(11):118-123.(In Chinese)

[11] Gao Jian,Optimal Design for Permanent Magnet Wind Power Generators Based on Converter Controlling Algorithm,Proceedings of the CSEE, vol. 28, no. 7, pp. 103-109, 2013

[12] Liu Xiangxiang, Li Xinyu, “Application of Variable Structure Control Strategy in Direct-Drive Permanent Magnet Synchronous Wind Turbine Generator”, Power System Technology, vol. 37, no. 2, 2012.